

Analysis of Force Transmission by a Knee Loading Device from Skin and Soft Tissue to Knee Joint Elements

Samson Rayi¹, Hiroki Yokata², Sohel Anwar¹

¹Department of Mechanical and Energy Engineering, Indiana University Purdue University Indianapolis (IUPUI), Indianapolis, IN, USA; ²Department of Biomedical Engineering, Indiana University Purdue University Indianapolis (IUPUI), Indianapolis, IN, USA

Correspondence to: Sohel Anwar, soanwar@iupui.edu

Keywords: Knee Loading, Modality, Loading Force, Bone Healing, Knee Rehabilitation, Finite Element Analysis

Received: March 16, 2019

Accepted: June 18, 2019

Published: June 21, 2019

Copyright © 2019 by authors and Scientific Research Publishing Inc.

This work is licensed under the Creative Commons Attribution-NonCommercial International License (CC BY-NC 4.0).

<http://creativecommons.org/licenses/by-nc/4.0/>



Open Access

ABSTRACT

Dynamic loading to a knee joint is considered to be an effective modality for enhancing the healing of long bones and cartilage that are subject to ailments like fractures, osteoarthritis, etc. We developed a knee loading device and tested it for force application. The device applies forces on the skin, whereas force transmitted to the knee joint elements is directly responsible for promoting the healing of bone and cartilage. However, it is not well understood how loads on the skin are transmitted to the cartilage, ligaments, and bone. Based on a CAD model of a human knee joint, we conducted a finite element analysis (FEA) for force transmission from the skin and soft tissue to a knee joint. In this study, 3D models of human knee joint elements were assembled in an FEA software package (SIMSOLID). A wide range of forces was applied to the skin with different thickness in order to obtain approximate force values transmitted from the skin to the joint elements. The maximum Von Mises stress and displacement distributions were estimated for different components of the knee joint. The results demonstrate that the high load bearing areas were located on the posterior portion of the cartilage. This prediction can be used to improve the design of the knee loading device.

1. INTRODUCTION

Human bone consists of rigid and dense connected tissues that are capable of repairing itself and adapt to stimuli such as various physical activities (walking, swimming, running, etc.). The strengthening or weakening of the bone tissues under such stimuli depends on weight, muscle strength, fitness, etc. [1]. A damaged bone tissue heals over time by body's natural healing process, which can be accelerated by ex-

ternal interferences such as mechanical loading under controlled conditions. The largest synovial joint in the human body is the knee joint that carries high loads. During the sitting, standing and climbing, it bears the weight of the body. Accordingly, it is highly susceptible to osteoarthritis and is one of the most injured parts of the human body. A lateral application of force on the knee joint was found effective in protecting bone tissue in the areas of distal femur and proximal tibia of the knee bone. The effects of the stimulation of bone regeneration are not limited to the applied areas but are seen along the length of the long bone [2]. When a specific loading force is applied to the epiphyses of the femur and tibia, the trabecular bone tissue, which is characterized by axial stress resistance, resists this force from the opposite direction. A human lower body bone structure is shown in **Figure 1** [3]. This results in reversible deformations in that area. These deformations create a variation of the fluid pressure in the intramedullary cavity. This pressure gradient allows the flow of fluids that carry essential nutrients to the bone cortex initiating osteoblast differentiation and osteogenesis thus helping in repair and regeneration of the bone tissue [2]. Thus such a knee loading regimen can be used as an effective treatment for bone rehabilitation as well as reducing the healing time of bone fractures and injuries. The lateral stress application is also less strenuous to the knee bone and reduces the amount of force that needs to be applied to get this result.

To our knowledge, few computational analyses are reported, which include not only cartilages but also the prominent ligaments such as anterior cruciate (ACL), posterior cruciate (PCL), medial collateral (MCL) and lateral collateral (LCL) as non-linear materials. Most previous studies used one-dimensional representations of the knee ligaments [4]. This simplified approach was proved to be useful for predicting joint kinematics but nonuniform three dimensional (3D) stresses and strains could not be predicted. Other researchers developed 3D finite element models of individual human ligaments such as the ACL [5] or the MCL [6]. Some papers presented specific computational models of parts of the human knee to discuss different aspects of its biomechanical behavior [7]. For instance, Heegard *et al.* [8] developed a 3D model to analyze the human biomechanics during passive knee flexion. In all these latter models, ligaments were modelled as nonlinear springs.

A prototype device was designed and built in the lab whose effectiveness still needs to be clinically tested on human subjects [9, 10]. **Figure 2** shows such a prototype device. This device has been validated to produce force levels of up to 40 N with a frequency of application of 5 Hz, which is the recommended value based on mice studies [11]. These forces are applied laterally on the soft tissues (skin, muscle, etc.) surrounding the knee joint, whereas the recommended force magnitudes are based on forces applied to the bone itself. Thus there is a need for analysis of forces transmitted from the knee loading device pads through the soft tissues to the knee joint bone and cartilage.

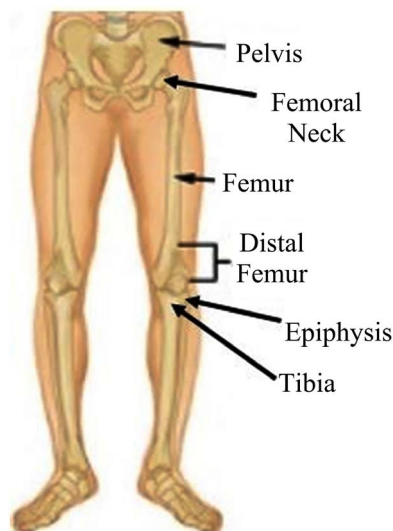
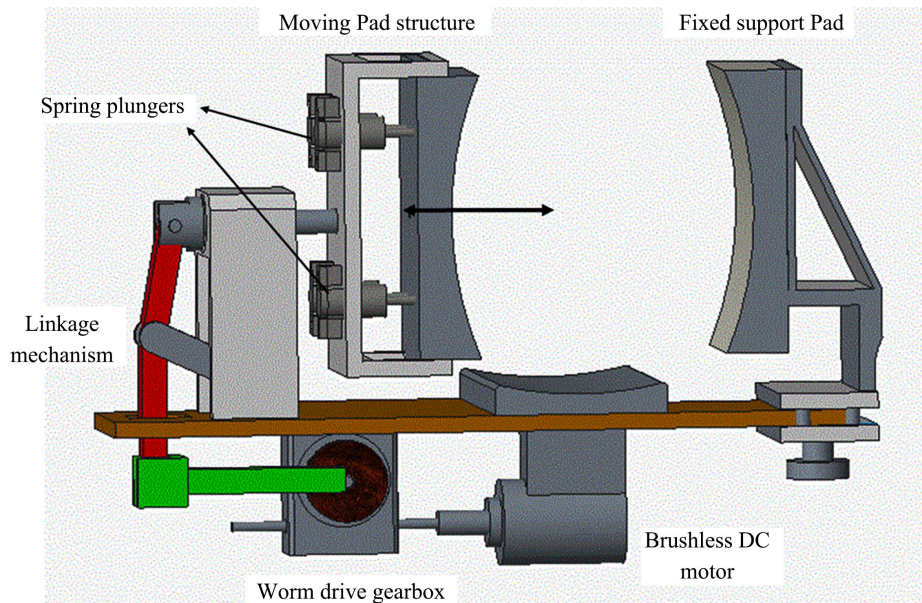
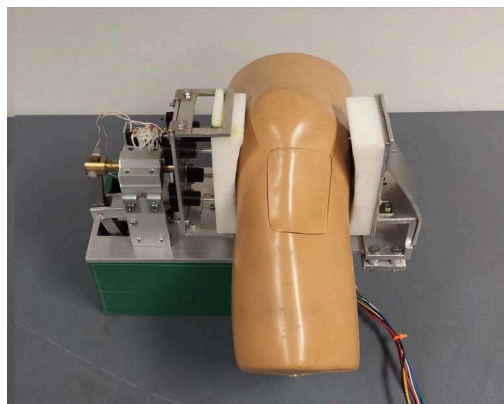


Figure 1. Brief anatomy of lower body bone structure of human body [3].



(a)



(b)

Figure 2. (a) Design details of the knee loading device; (b) Prototype of the design knee loading device.

Considerable efforts have been put into biomechanical modeling and computational analysis over the last few years [12-15]. Computational models present a standardized scheme for parametric studies, such as stress distributions for different geometries and kinematics. A finite element method is one of the computational techniques that has been extensively adopted to study biomechanics of the knee joint. Such analyses of the human knee joint can help in determining the underlying causes of cartilage degeneration that in turn results in osteoarthritis. The focus was to determine the effect of changes in the properties of bone joint on the stress and strain distribution in the knee joint. The soft tissues of the knee joint, namely the cartilages and ligaments, are particularly susceptible to wear owing to high levels of contact stresses. The main objective of this study is to determine the contact stresses in the knee joint due to the forces applied by a knee loading device.

We present here a complete 3D model of the healthy human knee joint. This included all the relevant ligaments and cartilage. Different experimental and numerical results were used to validate it. Once sufficiently validated, our main goal was to analyze the combined role of cartilage and ligaments in load transmission and stability.

2. KNEE MODEL

A practical model of the human knee generally consists of four bones, the femur, tibia, fibula, and patella, together with five ligaments that limit the movement between the bones. These ligaments, in addition, keep the bones at a specified distance, which is necessary for the correct function of the joint. A representative three dimensional geometric model of the knee structure was used for this work (Figure 3). The development of a knee joint three-dimensional geometric model is described in detail in [16, 17]. This work also includes the design of the skin model to study the forces transmitted through the skin and soft tissues. The skin model was designed using a CAD software Solidworks and was studied for force transmission analysis. The CAD design of the skin model developed in this work is shown in Figure 4.

For the analysis of the model, software package SIMSOLID was used. The assembled geometric models were input to the analysis module, and material properties were assigned to them. The different materials properties were used for the bone, cartilage, skin, and ligaments (Table 1) [18, 19]. All materials were assumed to be isotropic. The nonlinear stress-strain properties for these materials of the knee joint components are shown in Figures 5(a)-(d). Following the assignment of material properties to each individual geometric entity, appropriate constraints were applied to the assembly.

The stress-strain curves for the various materials are shown below:

Table 1. Material properties [18, 19].

Material	Poisson's ratio
Ligament	0.4
Cartilage	0.46
Bone	0.36
Skin	0.3

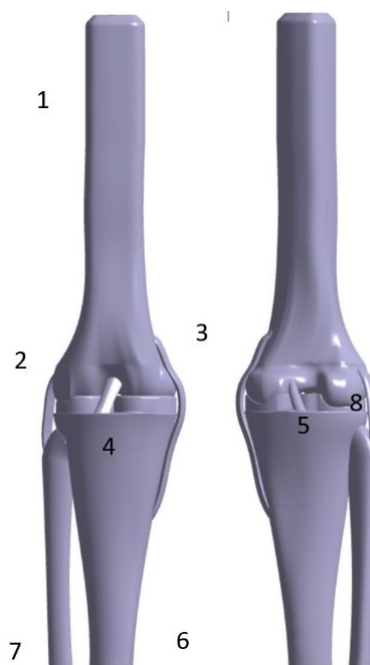


Figure 3. Knee model where (1) Femur; (2) Lateral collateral ligament (LCL); (3) Medial collateral ligament (MCL); (4) Anterior cruciate ligament (ACL); (5) Posterior cruciate ligament (PCL); (6) Tibia; (7) Fibula; (8) Cartilage.



Figure 4. Skin model.

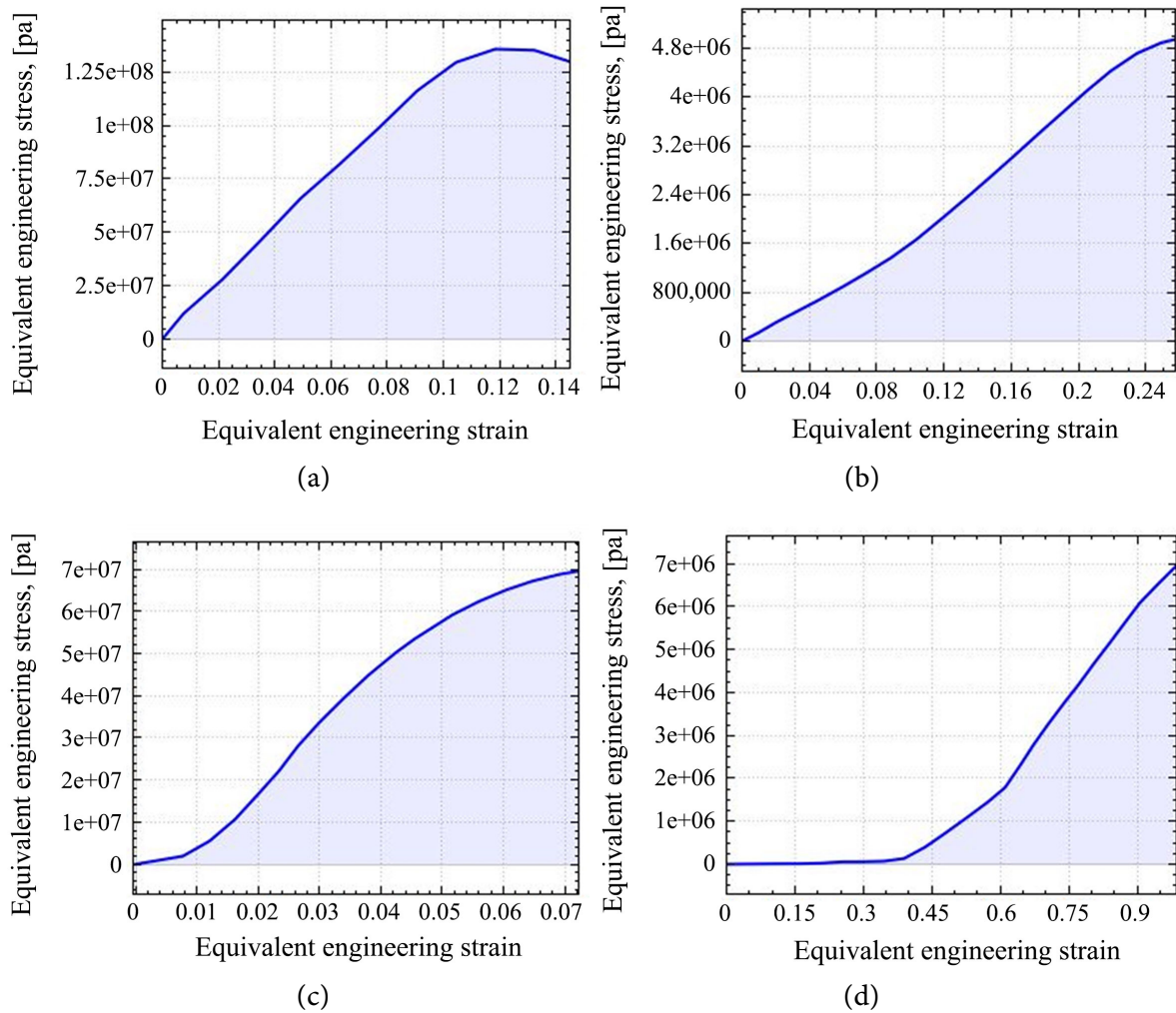


Figure 5. (a) Bone mechanical properties; (b) Cartilage mechanical properties; (c) Ligament mechanical properties; (d) Skin mechanical properties.

3. ANALYSIS FOR SKIN MODEL

The analysis for the skin model was performed in order to assess how the applied forces are transmitted from the skin to the knee joint components. It is challenging to develop the integrated 3D models with both hard and soft tissues due to major differences in their mechanical properties. The top and bottom surfaces of the skin model are constrained according to force loading conditions as applied by the knee loading device. A force was applied to the left side of the model, while the right side of the model was constrained with slider movement in order to emulate the force reaction on the right side. **Figure 9** shows the skin model with boundary conditions. The force magnitudes evaluated in this study are similar to the levels recommended for the portable knee loading device [10]. The development of this device is described in detail in a previous work [9, 10]. The values of different thicknesses and the different forces used in the analysis are shown in **Table 2**.

4. ANALYSIS FOR KNEE COMPONENTS

The automatic connections were used to represent the contact between bone and cartilage, between bone and ligament, and between the medial collateral ligament and the medial meniscus. The top and bottom surfaces of the tibia and femur were constrained in order to analyze the knee joint. The right side of the knee joint was constrained. The right side of the knee was also constrained. The forces obtained from skin model was applied to the left side of the knee joint. **Figure 6** also shows the model of the knee joint with boundary conditions. The analysis of the knee joint was performed with the given boundary conditions. The contact stresses were calculated for the entire model, but the focus was on the cartilage.

5. RESULTS AND DISCUSSION

The knee joint was mainly analyzed for the Von Mises stress (Maximum Equivalent Stress) and displacement magnitudes. The maximum Von Mises stress of $2.8077e-2$ [MPa] and the maximum Displacement of $2.4974e-3$ [MM] were located on the cartilage and tibia for a force magnitude of 33.80 N. **Figure 7(a)** and **Figure 7(b)** show the displacement and the Von Mises stress distributions on the knee joint components, respectively. **Figure 8(a)** and **Figure 8(b)** show the displacement and the Von Mises stress distributions on the femur. **Figure 9(a)** and **Figure 9(b)** show the displacement and the Von Mises stress distributions on the tibia, respectively. **Figure 10(a)** and **Figure 10(b)** show the displacement and the Von Mises stress distributions on the cartilage, respectively. **Figure 11(a)** and **Figure 11(b)** show the displacement and the Von Mises stress distributions on the ACL, respectively. **Figure 12(a)** and **Figure 12(b)** show the displacement and the Von Mises stress distributions on the fibula, respectively. **Figure 13(a)** and **Figure 13(b)** show the displacement and the Von Mises stress distributions for on the LCL, respectively. **Figure 14(a)** and **Figure 14(b)** show the displacement and the Von Mises stress distributions on the MCL, respectively. **Figure 15(a)** and **Figure 15(b)** show the displacement and the Von Mises stress distributions on the PCL, respectively.

In every case, the distribution of stress and strain on the model was similar. The maximum stress and strain appeared in the areas where the cartilage connected to the femur for every loading case. The results of this analysis for a soft tissue thickness of 1 mm and an applied force magnitude of 40 N are shown in **Table 3**. As can be seen from this analysis, the cartilage underwent the largest maximum displacement and maximum equivalent strain while tibia exhibited the largest maximum Von Mises stress. The stress-strain characteristics had linear response for both stress and strain analyses, where increased loads produce increased stresses and strains, for each type of load.

In order to study the effect of soft tissue thickness on the force transmission, three different soft tissue thicknesses were selected for finite element analysis. For each soft tissue thickness, three force magnitudes, as applied by the knee loading device, were considered: 20 N, 30 N, and 40 N. Finite element analysis of these force transmissions through the soft tissues with varying thickness are shown in **Table 4**.

A 3D model of the human knee was analyzed under a compressive force in this study. The main ob-

jective was to determine the contact stresses in the knee joint using analysis. Finite element analysis was used by other researchers to determine the distribution of compressive stresses in the healthy knee joint. Bendjaballah *et al.* [20] found that the compressive stress on the menisci varied between 1 MPa in the external periphery to 4 MPa in the internal periphery, under a compressive force of 1300 N. Dong *et al.* [21] obtained a compressive stress on the medial and lateral meniscus of 3.00 and 2.83 MPa, respectively. Pena *et al.* [22] found that the compressive stress on the medial meniscus was 3.31 MPa. The compressive stresses and displacement on the cartilage obtained in this study was $2.8077e-2$ [MPa] and $2.4974e-3$ [MM], respectively. The difference in the stress values may be due to the fact of low force values, and that frictionless nonlinear contact between the femoral and tibial cartilage, cartilage and menisci, and the femoral and patellar cartilage was not considered. The limitation of this study is that the knee joint components were assumed transversely isotropic. As it is shown in Figure 16, the model has a linear response, as it is expected, for both stress and strain analysis, where increased loads produce increased stresses and strains, for each type of load.

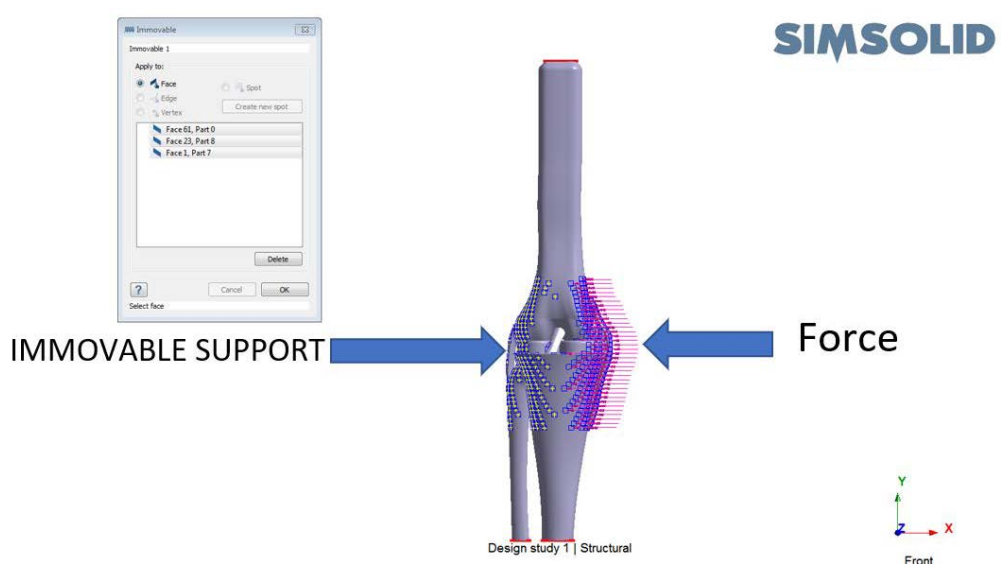


Figure 6. Skin and Knee Joint Model with boundary conditions.

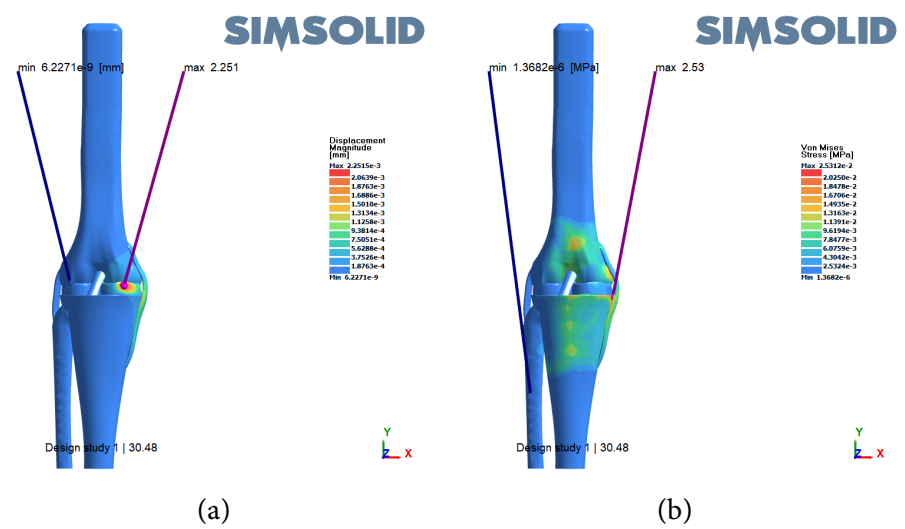


Figure 7. (a) Displacement magnitude for 33.8 N force; (b) Von Mises stress for 33.8 N force.

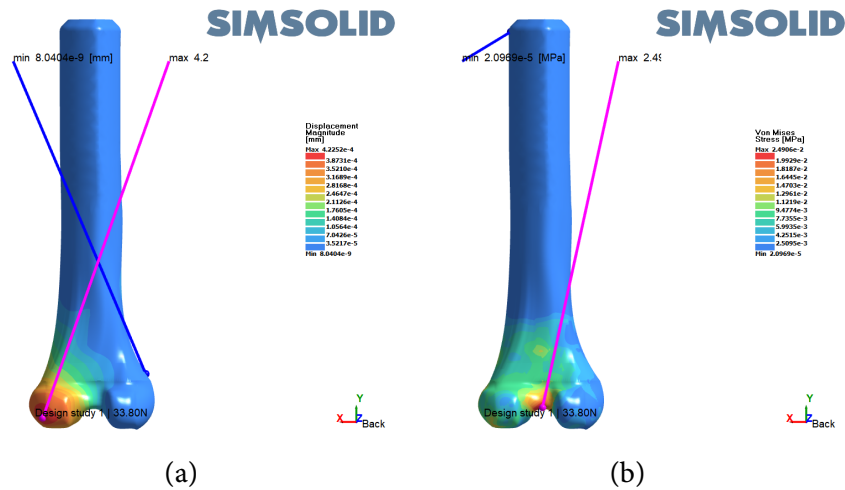


Figure 8. (a) Displacement for 33.8 N force on Femur; (b) Von Mises Stress for 33.8 N force on Femur.

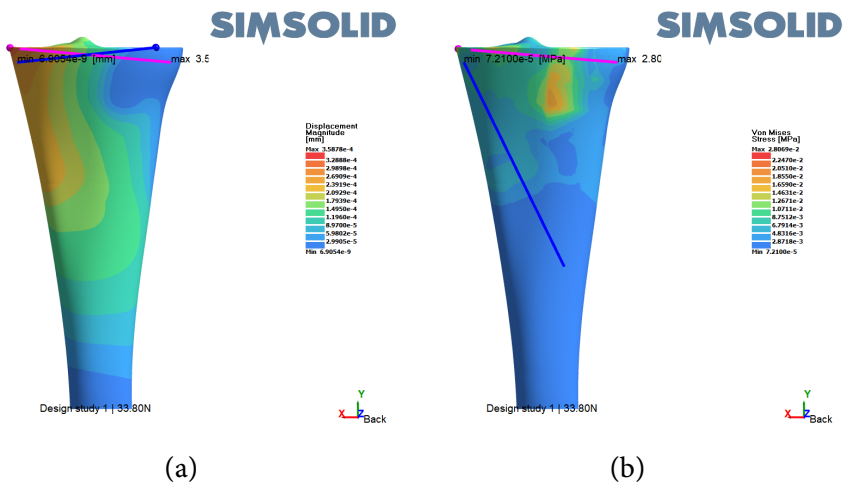


Figure 9. (a) Displacement for 33.8 N force on Tibia; (b) Von Mises Stress for 33.8 N force on Tibia.

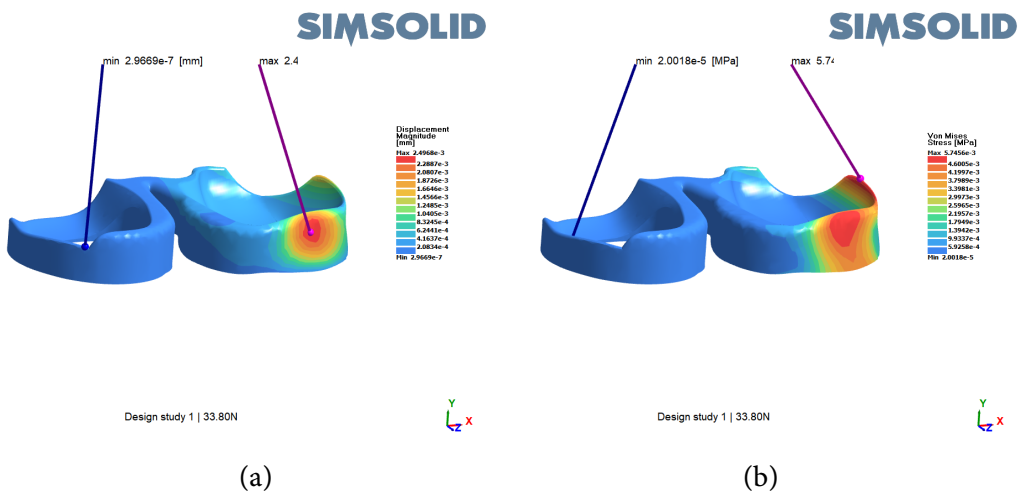


Figure 10. (a) Displacement for 33.8 N on Cartilage; (b) Von Mises Stress for 33.8 N on Cartilage.

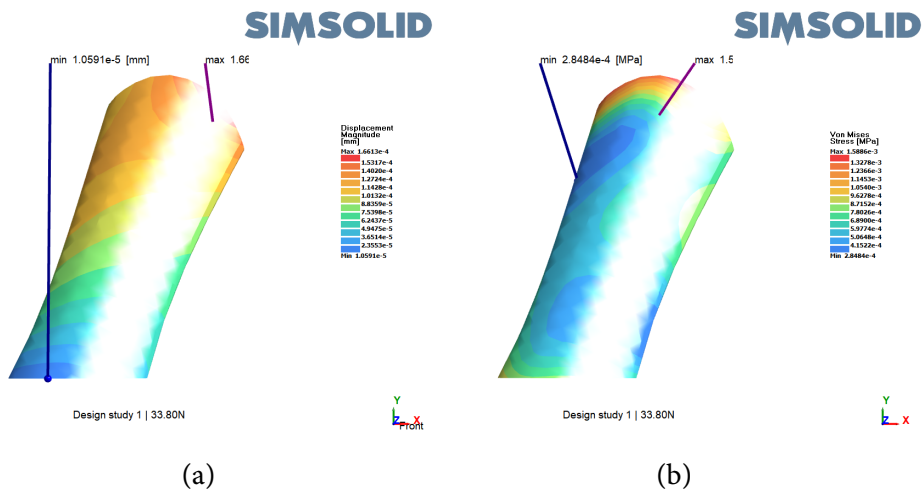


Figure 11. (a) Displacement for 33.8 N force on ACL; (b) Von Mises Stress for 33.8 N force on ACL.

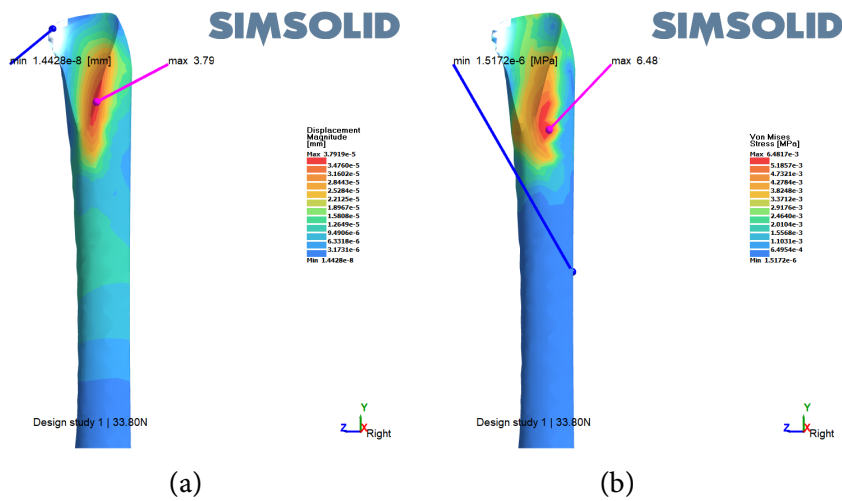


Figure 12. (a) Displacement for 33.8 N on Fibula; (b) Von Mises Stress for 33.8 N on Fibula.

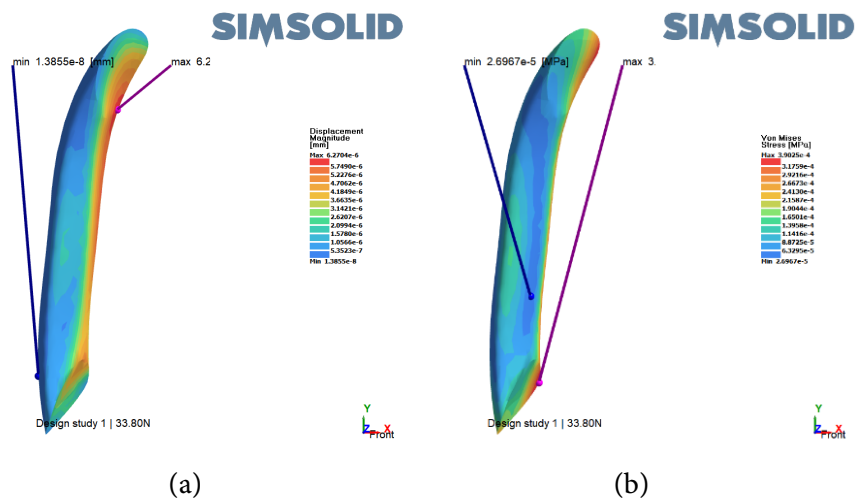


Figure 13. (a) Displacement for 33.8 N on LCL; (b) Von Mises Stress for 33.8 N on LCL.

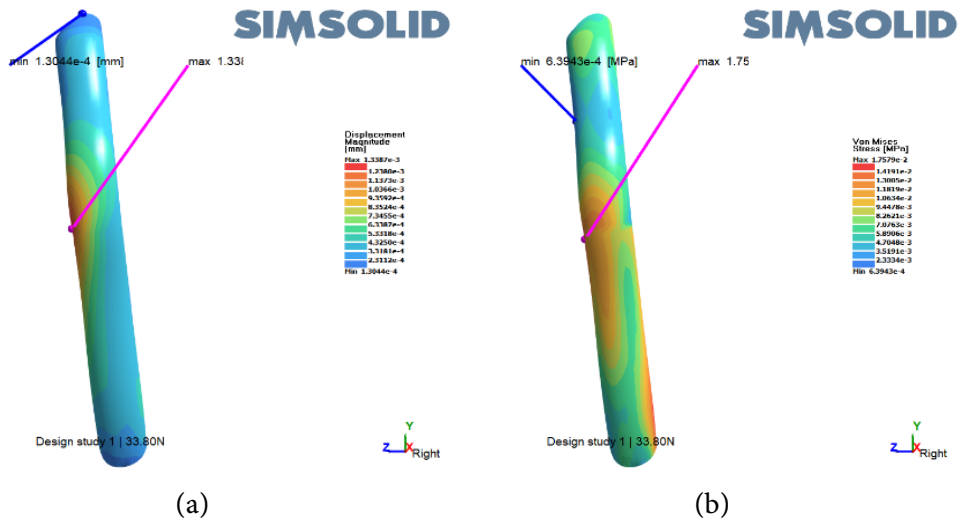


Figure 14. (a) Displacement for 33.8 N on MCL; (b) Von Mises Stress for 33.8 N on MCL.

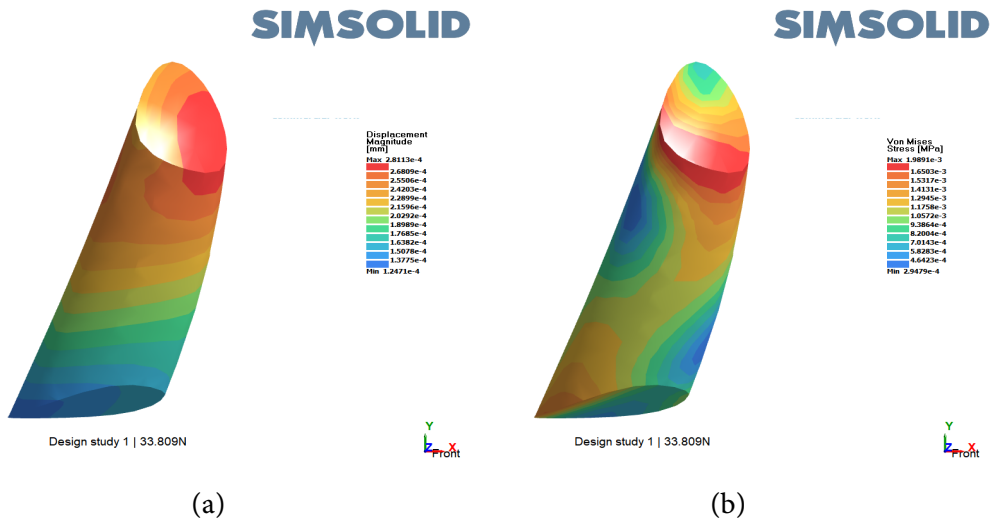
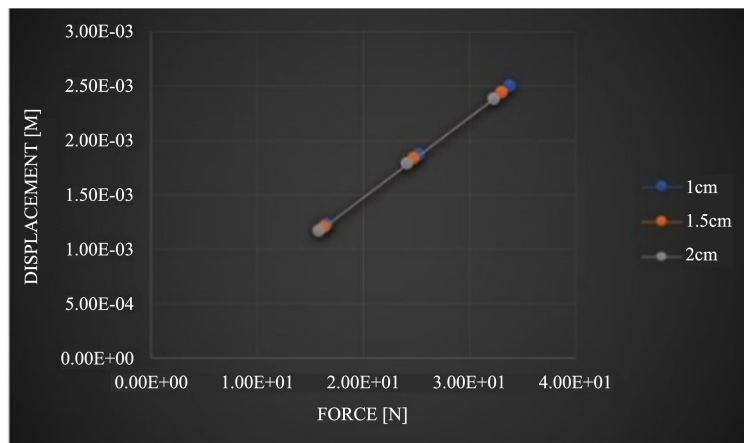
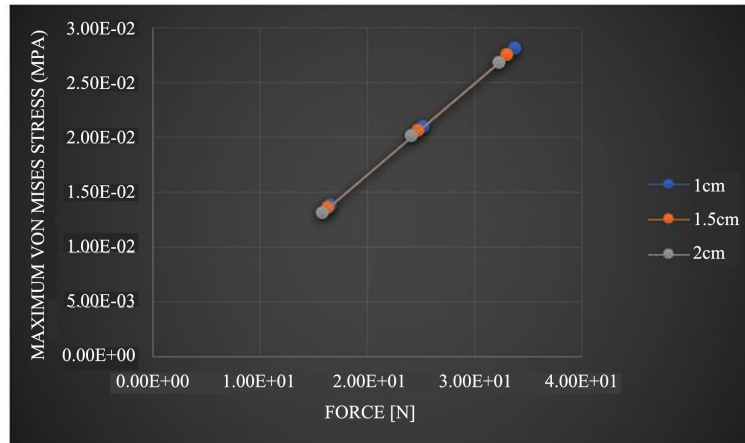


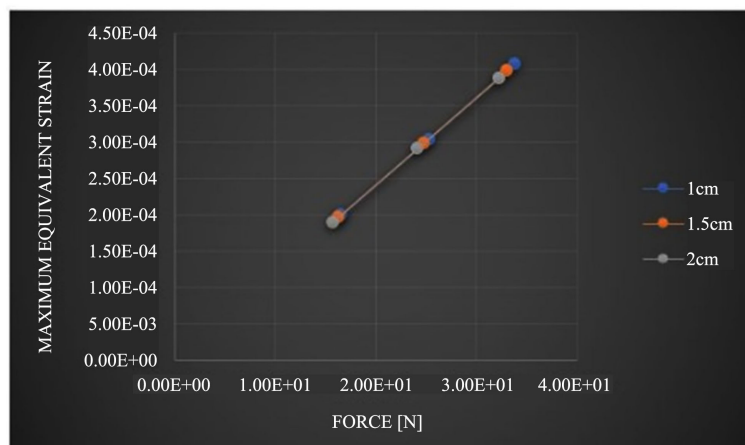
Figure 15. (a) Displacement for 33.8 N on PCL; (b) Von Mises Stress for 33.8 N on PCL.



(a)



(b)



(c)

Figure 16. (a) Force vs. Displacement; (b) Force vs. Stress; (c) Force vs. Strain.

Table 2. Forces and thickness used for the skin model.

Thickness of the Soft Tissue (cm)	Force on Left Side (N)	Force on Right Side (N)
1 cm	20 N	1.6591e+1 [N]
1 cm	30 N	2.5296e+1 [N]
1 cm	40 N	3.3809e+1 [N]
1.5 cm	20 N	1.6312e+1 [N]
1.5 cm	30 N	2.4819e+1 [N]
1.5 cm	40 N	3.3057e+1 [N]
2 cm	20 N	1.5824e+1 [N]
2 cm	30 N	2.4192e+1 [N]
2 cm	40 N	3.2305e+1 [N]

Table 3. Maximum stress and strain in each individual knee joint component.

Name	Force (N)	Maximum Displacement Magnitude (MM)	Maximum Von Mises Stress (MPa)	Maximum Equivalent Strain
Femur	3.3809e+1 [N]	4.2263e-4 [MM]	2.4913e-2 [MPa]	1.5725e-5
Tibia	3.3809e+1 [N]	3.5887e-4 [MM]	2.8077e-2 [MPa]	1.7722e-5
Cartilage	3.3809e+1 [N]	2.4974e-3 [MM]	5.7471e-3 [MPa]	4.0661e-4
ACL	3.3809e+1 [N]	2.8113e-4 [MM]	1.9891e-3 [MPa]	1.3483e-5
Fibula	3.3809e+1 [N]	3.7929e-5 [MM]	6.4834e-3 [MPa]	4.0923e-6
LCL	3.3809e+1 [N]	6.2720e-6 [MM]	3.9035e-4 [MPa]	2.6459e-6
MCL	3.3809e+1 [N]	1.3390e-3 [MM]	1.7583e-2 [MPa]	1.1918e-4
PCL	3.3809e+1 [N]	2.8113e-4 [MM]	1.9891e-3 [MPa]	1.3483e-5

Table 4. Maximum stress and strain on the cartilage for each load case.

Thickness of the Soft Tissue (cm)	Force (N)	Maximum Displacement Magnitude (MM)	Maximum Von Mises Stress (MPa)	Maximum Equivalent Strain
1 cm	1.6591e+1 [N]	1.2256e-3 [MM]	1.3778e-2 [MPa]	1.9954e-4
1 cm	2.5296e+1 [N]	1.8686e-3 [MM]	2.1007e-2 [MPa]	3.0423e-4
1 cm	3.3809e+1 [N]	2.4974e-3 [MM]	2.8077e-2 [MPa]	4.0661e-4
1.5 cm	1.6312e+1 [N]	1.2049e-3 [MM]	1.3546e-2 [MPa]	1.9618e-4
1.5 cm	2.4819e+1 [N]	1.8333e-3 [MM]	2.0611e-2 [MPa]	2.9849e-4
1.5 cm	3.3140e+1 [N]	2.4480e-3 [MM]	2.7521e-2 [MPa]	3.9857e-4
2 cm	1.5824e+1 [N]	1.1689e-3 [MM]	1.3141e-2 [MPa]	1.9031e-4
2 cm	2.4192e+1 [N]	1.7870e-3 [MM]	2.0090e-2 [MPa]	2.9095e-4
2 cm	3.2305e+1 [N]	2.3863e-3 [MM]	2.6828e-2 [MPa]	3.8852e-4

6. CONCLUSION

A 3D human knee joint model was built and analyzed under an axial compressive force, *i.e.* lateral force, which was generated with the knee loading device. Obviously, the model predicted that stresses, strains, and displacements elevated with increasing loads. The low and high load-bearing regions were estimated to be situated on the cartilage. According to several load case analyses for different values of direct loads, the solid model estimated stresses and strains within the elastic range. Furthermore, high stresses and strains were predicted to develop between the connections of soft and hard tissues. In particular, the results of this study demonstrated that the high load bearing areas were located on the posterior portion of the cartilages. It is expected that this prediction can be used to improve the design of the knee loading device.

ACKNOWLEDGEMENTS

This study was in part supported by a National Institute of Health (NIH) R01 grant number AR052144 (HY).

CONFLICTS OF INTEREST

The authors declare no conflicts of interest regarding the publication of this paper.

REFERENCES

1. Zhang, P., Malacinski, G.M. and Yokota, H. (2008) Joint Loading Modality: Its Application to Bone Formation and Fracture Healing. *British Journal of Sports Medicine*, **42**, 556-560. <https://doi.org/10.1136/bjism.2007.042556>
2. Su, M., Jiang, H., Zhang, P., Liu, Y., Wang, E., Hsu, A. and Yokota, H. (2006) Knee-Loading Modality Drives Molecular Transport in Mouse Femur. *Annals of Biomedical Engineering*, **34**, 1600-1606. <https://doi.org/10.1007/s10439-006-9171-z>
3. Barwick, J.F. and Nowotarski, P.J. (2016) Femur Shaft Fractures-Broken Thighbone. <https://orthoinfo.aaos.org/en/diseases--conditions/femur-shaft-fractures-broken-thighbone/>
4. Bendjaballah, M.Z., Shirazi-Adl, A. and Zukor, D.J. (1998) Biomechanical Response of the Passive Human Knee Joint under Anterior-Posterior Forces. *Clinical Biomechanics*, **13**, 625-633. [https://doi.org/10.1016/S0268-0033\(98\)00035-7](https://doi.org/10.1016/S0268-0033(98)00035-7)
5. Hirokawa, S. and Tsuruno, R. (2000) Three-Dimensional Deformation and Stress Distribution in an Analytical/Computational Model of the Anterior Cruciate Ligament. *Journal of Biomechanics*, **33**, 1069-1077. [https://doi.org/10.1016/S0021-9290\(00\)00073-7](https://doi.org/10.1016/S0021-9290(00)00073-7)
6. Gardiner, J., Weiss, J. and Rosenberg, T. (2001) Strain in the Human Medial Collateral Ligament during Valgus Loading of the Knee. *Clinical Orthopaedics and Related Research*, **391**, 266-274. <https://doi.org/10.1097/00003086-200110000-00031>
7. Eijden, T.M.V., Kouwenhoven, E., Verbug, J. and Weijs, W.A. (1986) A Mathematical Model of the Patellofemoral Joint. *Journal of Biomechanics*, **19**, 219-229. [https://doi.org/10.1016/0021-9290\(86\)90154-5](https://doi.org/10.1016/0021-9290(86)90154-5)
8. Heegard, J., Leyvraz, P.F., Curnier, A., Rakotomana, L. and Huiskes, R. (1995) The Biomechanics of the Human Patella during Passive Knee Flexion. *Journal of Biomechanics*, **28**, 1265-1279. [https://doi.org/10.1016/0021-9290\(95\)00059-Q](https://doi.org/10.1016/0021-9290(95)00059-Q)
9. Prabhala, S.K., Chien, S., Yokota, H. and Anwar, S. (2016) A Mechatronic Loading Device to Stimulate Bone Growth via a Human Knee. *Sensors*, **16**, 1615. <https://doi.org/10.3390/s16101615>
10. Fitzwater, D., Dodge, T., Chien, S., Yokota, H. and Anwar, S. (2013) Development of a Portable Knee Rehabilitation Device that Uses Mechanical Loading. *Journal of Medical Devices*, **7**, Article ID: 041007. <https://doi.org/10.1115/1.4024830>
11. Hamamura, K., Zhang, P., Zhao, L., Shim, J.W., Chen, A., Dodge, T.R., Sun, H.B., *et al.* (2013) Knee Loading Reduces MMP13 Activity in the Mouse Cartilage. *BMC Musculoskeletal Disorders*, **14**, 312. <https://doi.org/10.1186/1471-2474-14-312>
12. Bendjaballah, M., Shirazi-Adl, A. and Zukor, D.J. (1997) Finite Element Analysis of Human Knee Joint in Varus-Valgus. *Clinical Biomechanics*, **12**, 139-148. [https://doi.org/10.1016/S0268-0033\(97\)00072-7](https://doi.org/10.1016/S0268-0033(97)00072-7)
13. Kazemi, M., Dabiri, Y. and Li, L.P. (2013) Recent Advances in Computational Mechanics of the Human Knee Joint. *Computational and Mathematical Models in Medicine*, **2013**, Article ID: 718423. <https://doi.org/10.1155/2013/718423>

14. Vairis, A., Petousis, M., Stefanoudakis, G., Vidakis, N., Kandyla, B. and Tsainis, A.M. (2013) Studying the Intact, ACL-Deficient and Reconstructed Human Knee Joint Using a Finite Element Model. *ASME 2013 International Mechanical Engineering Congress and Exposition*, San Diego, CA, 15-21 November 2013, V03AT03A060-V03AT03A060.
15. Beynnon, B., Yu, J., Huston, D., Fleming, B., Johnson, R., Haugh, L. and Pope, M. (1996) A Sagittal Plane Model of the Knee and Cruciate Ligaments with Application of a Sensitivity Analysis. *ASME Journal of Biomechanical Engineering*, **118**, 227-239. <https://doi.org/10.1115/1.2795965>
16. Petousis, M., Vairis, A., Yfanti, S., Kandyla, B. and Chrysoulakis, C. (2011) Study of a 3D Knee Model. *7th International Conference on New Horizons in Industry, Business and Education*, Chios Island, Greece, 25-26 August, 2011, 281-287.
17. John, D., Pinisetty, D. and Gupta, N. (2013) Image-Based Model Development and Analysis of the Human Knee Joint. In: Andreaus, U. and Iacoviello, D. Eds., *Biomedical Imaging and Computational Modeling in Biomechanics. Lecture Notes in Computational Vision and Biomechanics*, Springer, Dordrecht, 55-79. https://doi.org/10.1007/978-94-007-4270-3_4
18. Silver, F.H., Freeman, J.W. and DeVore, D. (2001) Viscoelastic Properties of Human Skin and Processed Dermis. *Skin Research and Technology*, **7**, 18-23. <https://doi.org/10.1034/j.1600-0846.2001.007001018.x>
19. Pal, S. (2014) Mechanical Properties of Biological Materials. In: *Design of Artificial Human Joints & Organs*, Springer, Boston, MA, 23-40. https://doi.org/10.1007/978-1-4614-6255-2_2
20. Bendjaballah, M.Z., Shirazi-Adl, A. and Zukor, D.J. (1995) Biomechanics of the Human Knee Joint in Compression: Reconstruction, Mesh Generation and Finite Element Analysis. *The Knee*, **2**, 69-79. [https://doi.org/10.1016/0968-0160\(95\)00018-K](https://doi.org/10.1016/0968-0160(95)00018-K)
21. Dong, Y., Hu, G., Dong, Y., Hu, Y. and Xu, Q. (2014) The Effect of Meniscal Tears and Resultant Partial Meniscectomies on the Knee Contact Stresses: A Finite Element Analysis. *Computer Methods in Biomechanics and Biomedical Engineering*, **17**, 1452-1463. <https://doi.org/10.1080/10255842.2012.753063>
22. Peña, E., Calvo, B., Martínez, M.A., Palanca, D. and Doblaré, M. (2005) Finite Element Analysis of the Effect of Meniscal Tears and Meniscectomies on Human Knee Biomechanics. *Clinical Biomechanics*, **20**, 498-507. <https://doi.org/10.1016/j.clinbiomech.2005.01.009>